THE JOURNAL OF BIOLOGICAL CHEMISTRY VOL. 291, NO. 8, pp. 3990–4003, February 19, 2016

Cytochrome P450 17A1 Interactions with the FMN Domain of Its Reductase as Characterized by NMR*

Received for publication, July 6, 2015, and in revised form, December 29, 2015 Published, JBC Papers in Press, December 30, 2015, DOI 10.1074/jbc.M115.677294

D. Fernando Estrada‡, Jennifer S. Laurence§1, and Emily E. Scott‡2

From the ‡Department of Medicinal Chemistry, University of Kansas, Lawrence, Kansas 66045 and the §Department of Pharmaceutical Chemistry, University of Kansas, Lawrence, Kansas 66047

To accomplish key physiological processes ranging from drug metabolism to steroidogenesis, human microsomal cytochrome P450 enzymes require the sequential input of two electrons delivered by the FMN domain of NADPH-cytochrome P450 reductase. Although some human microsomal P450 enzymes can instead accept the second electron from cytochrome b_5, for human steroidogenic CYP17A1, the cytochrome P450 reductase FMN domain delivers both electrons, and b_5 is an allosteric modulator. The structural basis of these key but poorly understood protein interactions was probed by solution NMR using the catalytically competent soluble domains of each protein. Formation of the CYP17A1·FMN domain complex induced differential line broadening of the NMR signal for each protein. Alterations in the exchange dynamics generally occurred for residues near the surface of the flavin mononucleotide, including 87–90 (loop 1), and for key CYP17A1 active site residues. These interactions were modulated by the identity of the substrate in the buried CYP17A1 active site and by b_5. The FMN domain outcompetes b_5 for binding to CYP17A1 in the three-component system. These results and comparison with previous NMR studies of the CYP17A1·b_5 complex suggest a model of CYP17A1 enzyme regulation.

Numerous microsomal cytochrome P450 enzymes play key roles in human drug metabolism and the biosynthesis, interconversions, and degradation of hormones, vitamins, fatty acids, and bile acids. These reactions are all critically dependent on a single multidomain NADPH-cytochrome P450 oxidoreductase (CPR)[3] enzyme (1). CPR is required to donate the first electron required for cytochrome P450 catalysis, but frequently it also performs a second reduction of P450 required for substrate monooxygenation (2). The N terminus of CPR forms a membrane-spanning anchor that co-localizes reductase to the endoplasmic reticulum (3, 4) alongside microsomal P450 enzymes. The remainder of CPR consists of two flavin-binding domains separated by a linker domain and a flexible hinge. One domain of CPR contains the binding sites for the NADPH-reducing agent and the flavin adenine nucleotide (FAD) cofactor that initially accepts electrons from NADPH, whereas the N-terminal domain binds the flavin mononucleotide (FMN) cofactor that accepts electrons from FAD and transfers them to the P450. In initial structures of CPR (4), the FAD and FMN were closely associated in space, an arrangement supporting efficient FAD-to-FMN electron transfer, but a conformation that precludes FMN-to-P450 electron transfer. Later structures of a CPR mutant with a deletion in the linker region revealed several different conformations of CPR in which the FMN domain was exposed and would be available for electron delivery to P450 (5). It has been proposed that CPR oscillates between these states during its electron delivery cycle (5–9). Although interactions between CPR and a given P450 enzyme may involve some hydrophobic contributions (10), the primary factors are thought to consist of charge pairing interactions between the anionic surface of the FMN domain and cationic surface residues on the proximal side (nearest the axial heme coordination) of P450 enzymes (11–13).

Such electrostatically mediated protein interactions and subsequent electron transfer from the CPR FMN domain to human cytochrome P450 17A1 (CYP17A1) (14, 15) support two distinct steroidogenic reactions as follows: 1) hydroxylation of pregnenolone or progesterone at the carbon 17 position; and 2) a 17,20-lyase reaction in which 17α-hydroxypregnenolone is converted into the initial androgen, dehydroepiandrosterone (16). The former reaction is necessary for human production of glucocorticoids and sex steroids and is little affected by the presence of the small heme-containing protein cytochrome b_5. In contrast, the subsequent lyase reaction required only for androgen and estrogen biosynthesis is significantly enhanced by the presence of the b_5, which acts allosterically without apparent transfer of electrons in the CYP17A1 system (14, 15). The structural nature of the complex interactions between human (membrane) P450 enzymes, CPR, and b_5 is poorly understood, in part because no x-ray structures are available of these complexes, although cross-linking and mutagenesis studies have made key contributions (13, 17–20), and a structure is available of a soluble bacterial P450 with its redox partner (21).

Recently, solution protein NMR has been used to evaluate P450 interactions with its partner catalytic proteins (22–24). Such studies demonstrated that the presence and identity of a ligand in the CYP17A1 active site altered [^{15}N]b_5 binding and that b_5 and CPR binding to CYP17A1 are mutually exclusive (23). More recently, b_5 binding was found to induce a redistri-

* This work was supported by National Institutes of Health Grants F32 GM103069 (to D. F. E.) and GM102505 (to E. E. S.). The authors declare that they have no conflicts of interest with the contents of this article. The content is solely the responsibility of the authors and does not necessarily represent the official views of the National Institutes of Health.

[1] To whom correspondence may be addressed: Dept. of Pharmaceutical Chemistry, University of Kansas, MRB, 2030 Becker Dr., Lawrence, KS 66047. Tel.: 785-865-3405; E-mail: laurencj@ku.edu.

[2] To whom correspondence may be addressed: Dept. of Medicinal Chemistry, University of Kansas, 1251 Wescoe Hall Dr., Lawrence, KS 66045. Tel.: 785-864-5559; Fax: 785-864-5326; E-mail: eescott@ku.edu.

[3] The abbreviations used are: CPR, cytochrome P450 oxidoreductase; CYP, cytochrome P450; b_5, cytochrome b_5; Ni-NTA, nickel-nitrilotriacetic acid.

bution of slowly exchanging [^{15}N]CYP17A1 backbone conformations, specifically in regions of the protein forming the "roof" of the active site that is likely flexible for substrate entry (24). Although these studies have provided important new insights primarily into the b_5·CYP interaction, the corresponding perspective on CYP17A1 interaction with CPR has been little investigated.

The sizes of CPR (76.7 kDa) and CYP17A1 (57.4 kDa), the membrane nature of both proteins, and the presumed cycling of CPR between conformational states, all make solution NMR studies of the complex (134.1 kDa) challenging. Thus, this NMR study probes such interactions by employing CYP17A1 with the N-terminal transmembrane helix deleted (55.6 kDa) and the isolated FMN domain of CPR (21.5 kDa). This truncated CYP17A1 performs both hydroxylase and lyase reactions (25). The isolated FMN domain has the same structure as within full-length CPR, can accept electrons from the isolated FAD domain (3–5, 26), and can transmit them to a P450 (27, 28). This simplified system permits detailed NMR studies of the various protein interactions. Interactions between the FMN domain and CYP17A1 induced line broadening for residues on both proteins, consistent with an interaction in the intermediate chemical exchange time regime. A contiguous stretch of resonances for FMN domain residues 87–90, which compose loop 1 of the FMN binding pocket, were modestly more broadened than the average, consistent with this region interacting with CYP17A1. Differences were observed in the extent of such line broadening when CYP17A1 contained the 17α-hydroxylase substrate (pregnenolone) *versus* the 17,20-lyase substrate (17α-hydroxypregnenolone) in its active site. CYP17A1 substrates also modulated the ability of the FMN domain to compete for and disrupt the CYP17A1·b_5 complex. Overall, FMN domain line broadening was more pronounced than observed for b_5 when equivalent amounts of CYP17A1 were added, suggesting that CYP17A1 has a higher affinity for FMN domain than b_5. Integration of these results with previous structure and function information suggests a cohesive model for modulation of CYP17A1 as required to generate not only the male androgenic and female estrogenic sex steroids but also glucocorticoids.

Experimental Procedures

Protein Expression and Purification—DNA encoding the human CPR FMN binding domain (residues 62–241) fused to a C-terminal His_6 tag was synthesized and inserted into the pET-15b expression vector (GenScript, Piscataway, NJ). The resulting construct was similar to one used previously for both NMR and crystallographic studies (26, 29) except that the His tag was repositioned from the N to C terminus. This plasmid was transformed into chemically competent *Escherichia coli* BL21(DE3) cells and selected in all subsequent cultures by incorporating ampicillin (50 μg/ml). A single colony grown overnight at 37 °C on a lysogeny broth (LB) agar plate was inoculated into 10 ml of liquid LB and grown at 37 °C with shaking (250 rpm) for 8 h. Fifty μl of this small scale culture were used to inoculate a 1-liter flask containing 200 ml of LB. After shaking at 250 rpm and 37 °C overnight (~15 h), 10 ml of this culture was used to inoculate 1 liter of terrific broth in a 2.8-liter Fernbach flask. The cells were grown at 37 °C with shaking at 250 rpm until the absorbance at 600 nm reached ~0.6–0.8. Expression of the CPR FMN domain was then induced with 25 mg of isopropyl β-D-1-thiogalactopyranoside per liter of culture, and riboflavin (35 mg/liter, Sigma) was added to facilitate adequate flavin cofactor production. Following induction, the shaking was reduced to 180 rpm, and the temperature was reduced to 25 °C. Expression continued for 16 h, at which point cells were harvested by centrifugation at 6,800 × *g* for 10 min. Cell pellets were resuspended in Ni-NTA binding buffer (20 mM Tris-HCl, 0.3 M NaCl, 5 mM imidazole, 60 μg/ml phenylmethylsulfonyl fluoride, pH 7.9) and either stored at −80 °C or subjected to a freeze/thaw cycle for same-day purification. Cells were lysed via sonication on ice for 30 s bursts for a total of 3 min. Lysate was then centrifuged for 30 min at 104,000 × *g* at 4 °C. The supernatant was loaded onto a column containing 30 ml of charged Ni-NTA Superflow resin (Qiagen, Venlo, Netherlands) pre-equilibrated with Ni-NTA-binding buffer. The column was subsequently washed with 60 ml of additional binding buffer and 180 ml of wash buffer (20 mM Tris-HCl, 0.3 M NaCl, 50 mM imidazole, pH 7.9), followed by elution with 20 mM Tris-HCl, 0.3 M NaCl, 5 μM FMN, 200 mM imidazole, pH 7.9. Eluted protein was pooled, concentrated to 1 ml using an Amicon centrifugal filter unit (EMD Millipore, Darmstadt, Germany), and loaded on a Superdex 200 resin (GE Healthcare). This column had been pre-equilibrated with 20 mM Tris-HCl, 0.3 M NaCl, 5 μM FMN, 0.2 mM dithiothreitol, 0.02 mM EDTA, pH 7.9, and subsequently run with the same buffer for 1.5 column volumes at 1 ml/min. Purified FMN domain eluted ~89 ml, consistent with the expected molecular mass for the monomeric protein (21.5 kDa). Purity was evaluated by SDS-PAGE. Protein concentration was measured using the bicinchoninic acid assay (Pierce). Production of FMN domain uniformly labeled with ^{15}N was carried out as described above, except that minimal media containing $^{15}NH_4Cl$ was used during expression.

The expression construct for the soluble heme-containing domain of cytochrome b_5 (residues 1–108) was generated by substituting the nucleotide sequence coding for the 26 amino acids of its C-terminal transmembrane helix with that encoding a His_6 tag (13.1 kDa). Expression and purification were as described previously (23), but with the addition of heme in early stages to facilitate holoprotein generation (30).

CYP17A1 was expressed omitting the 19 amino acids composing its N-terminal transmembrane helix and purified as described for unlabeled (23, 31) and ^{15}N-labeled (24) samples. Generation of the CYP17A1 point mutants R347Q, R358H, and R449L was carried out as described previously (23), but with substitution of the substrate pregnenolone for the inhibitor abiraterone during expression and purification.

Generation of [^{13}C,^{2}H,^{15}N]CYP17A1 for three-dimensional data collection was carried out as follows. The CYP17A1 plasmid was transfected into *E. coli* strain NCM533 (Kan^R) (gift of Tom Pochapsky) along with the GroEL and GroES chaperone plasmid pG-KJE8 (Takara Bio, Kyoto, Japan). Culture volumes were scaled up along with acclimatization of increasing D_2O concentrations until a volume of 250 ml of 70% D_2O was reached, centrifuged, and resuspended into 500 ml of 99% D_2O containing [^{15}N] NH_4Cl. Subsequently, cultures were scaled up

to 1 liter of 99% D_2O. Minimal media components were similar to those described previously for CYP17A1 (24) but supplemented with 0.5 g/liter [^{13}C,^{2}H,^{15}N]ISOGRO complex growth media (Sigma) and [^{13}C,^{2}H]glucose (Sigma). Cells were grown to log phase, induced, and allowed to express for 72 h at 37 °C and 180 rpm. Upon harvesting, purification of CYP17A1 proceeded as described previously (24).

Titrations of CYP17A1 and the FMN Domain—Isotopically labeled and unlabeled FMN domain, CYP17A1, or b_5 proteins were individually exchanged into NMR buffer consisting of 50 mM potassium phosphate, 50 mM NaCl, and 10% D_2O, pH 6.5. When FMN domain is present, 0.2 mM dithiothreitol, 0.02 mM EDTA, and 0.4 mM FMN were also added to the NMR buffer. When substrate or inhibitor-saturated CYP17A1 was used, 50 μM excess ligand was added just prior to the NMR experiment. Each sample was made immediately prior to data collection by combining [^{15}N]FMN domain at a constant concentration 0.1 mM, and various concentrations of CYP17A1 and/or b_5 on ice. Protein mixtures were then transferred into a thin walled 5-mm NMR sample tube (Wilmad LabGlass, Vineland, NJ) at a final volume of 400 μl. Samples for titration of [^{15}N]CYP17A1 with unlabeled FMN domain were prepared similarly, but with 0.2 mM labeled CYP17A1 and 10 μM abiraterone (inhibitor).

CYP17A1 Assignments and NMR Spectroscopy—All two-dimensional NMR spectra were acquired on a Bruker Avance 800 MHz spectrometer with a cryogenically cooled triple resonance (^{1}H, ^{15}N, and ^{13}C) probe at the University of Kansas Biomolecular NMR Core Laboratory. All three-dimensional data were acquired on a Bruker Avance 800 MHz spectrometer at the NMR Facility at Brandeis University. Acquisition temperatures were 25 °C for ^{1}H-^{15}N HSQC spectra of the FMN domain and b_5 and three-dimensional data on CYP17A1 with abiraterone and 35 °C for two-dimensional ^{1}H-^{15}N TROSY HSQC spectra of CYP17A1 during titrations. The two-dimensional spectra of the FMN domain and b_5 were acquired using 80 scans and 100 increments, and 72 scans with 128 increments for CYP17A1. Spectra were processed with NMRPipe (32) and analyzed using NMRView (33) for two-dimensional spectra or Topspin (Bruker, Billerica, MA) and CCPNMR (34) for three-dimensional data. Backbone assignments for b_5 and the FMN domain of CPR have been reported previously (7, 29, 35) as Biological Magnetic Resonance Data Bank entries 6921 and 19,301, respectively. Approximately 75% of the reported FMN domain assignments were clearly transferable onto the ^{1}H-^{15}N HSQC spectra collected for this study. Partial assignment of the CYP17A1 backbone was carried out using a combination of ^{1}H-^{15}N TROSY HSQC (36) spectra with selective labeling of particular residues (Leu, Val, Ile, Ala, and Phe) and data from the three-dimensional experiments TRHNCA (37, 38), TRHNCACB (38), TRHNCACO (38), and N-NOESY of CYP17A1 in complex with abiraterone.

Results

Summary of P450/Ligand/CPR/b_5 System under Study—In humans, microsomal NADPH-cytochrome P450 reductase and cytochrome b_5 proteins interact with cytochrome P450 enzymes, although all three integral membrane proteins are anchored on the surface of the endoplasmic reticulum. Truncation of CPR and b_5 to remove their terminal transmembrane helices yields soluble proteins (35, 39). Human P450 enzymes truncated in this manner retain a monofacial membrane interaction but can be extracted with detergent. Combination of truncated CYP17A1 and truncated CPR proteins in solution forms a catalytic system capable of substrate metabolism with wild type regio- and stereoselectivity (25, 39). At the same time this increases protein expression, facilitating the protein quantities required for structural work, and reduces nonspecific hydrophobic interactions between the transmembrane helices in solution, facilitating analysis of interactions between the catalytic domains. To permit examination of the complex structural interactions among these three proteins by solution NMR, further simplification was employed in this study by using only the FMN domain of CPR responsible for electron delivery to P450. This approach is supported by NMR and x-ray experiments previously demonstrating that the structure of the isolated FMN domain is very similar to its structure when part of the larger multidomain CPR and regardless of which conformational state the CPR adopts (3–5, 26). Functionally, the isolated FMN domain is also capable of accepting electrons from the isolated FAD domain of CPR (27, 40) and delivering those electrons to P450 to support catalysis, as demonstrated by metabolism of 7-ethoxyresorufin by CYP1A1 in a reconstituted system consisting of the three proteins (27).

To validate that the isolated FMN domain is capable of facilitating catalysis in CYP17A1, hydroxylase assays were performed with CYP17A1, CPR, and substrate, in the absence and presence of increasing concentrations of the isolated FMN domain. Consistent with the previously reported CYP1A1 data, addition of the isolated FMN domain caused linear increases in pregnenolone and progesterone hydroxylation (data not shown).

In the following discussion of multiple protein and ligand complexes, the name of the P450 followed by the name of a ligand in parentheses (*e.g.* CYP17A1(pregnenolone)) is used to indicate the P450 saturated with the indicated ligand, and the names of two proteins separated by a bullet (*e.g.* CYP17A1·FMN) indicates a complex between them. Combinations such as CYP17A1(pregnenolone)·FMN indicate a complex formed between CYP17A1 saturated with the substrate pregnenolone and the CPR FMN domain. When molar ratios of these proteins are discussed (*e.g.* 1:1), the first number indicates the relative concentration of CYP17A1, and the second number refers to the relative concentration of either FMN or b_5 (when only two proteins are present) and CYP17A1:FMN:b_5 when all three proteins are present. The isotopically labeled protein differs between the experiments discussed herein and so will be explicitly noted [^{15}N] throughout.

Finally, because the different labeled proteins have different intrinsic dynamics, the temperatures at which different experiments were undertaken were empirically determined as those that best revealed changes upon titration. When the much smaller b_5 and FMN domain proteins were isotopically labeled and used as reporters of the interactions, data were collected at 25 °C. When the much larger CYP17A1 protein was isotopically labeled, this temperature was 35 °C. Unless noted, no significant differences were observed at different temperatures.

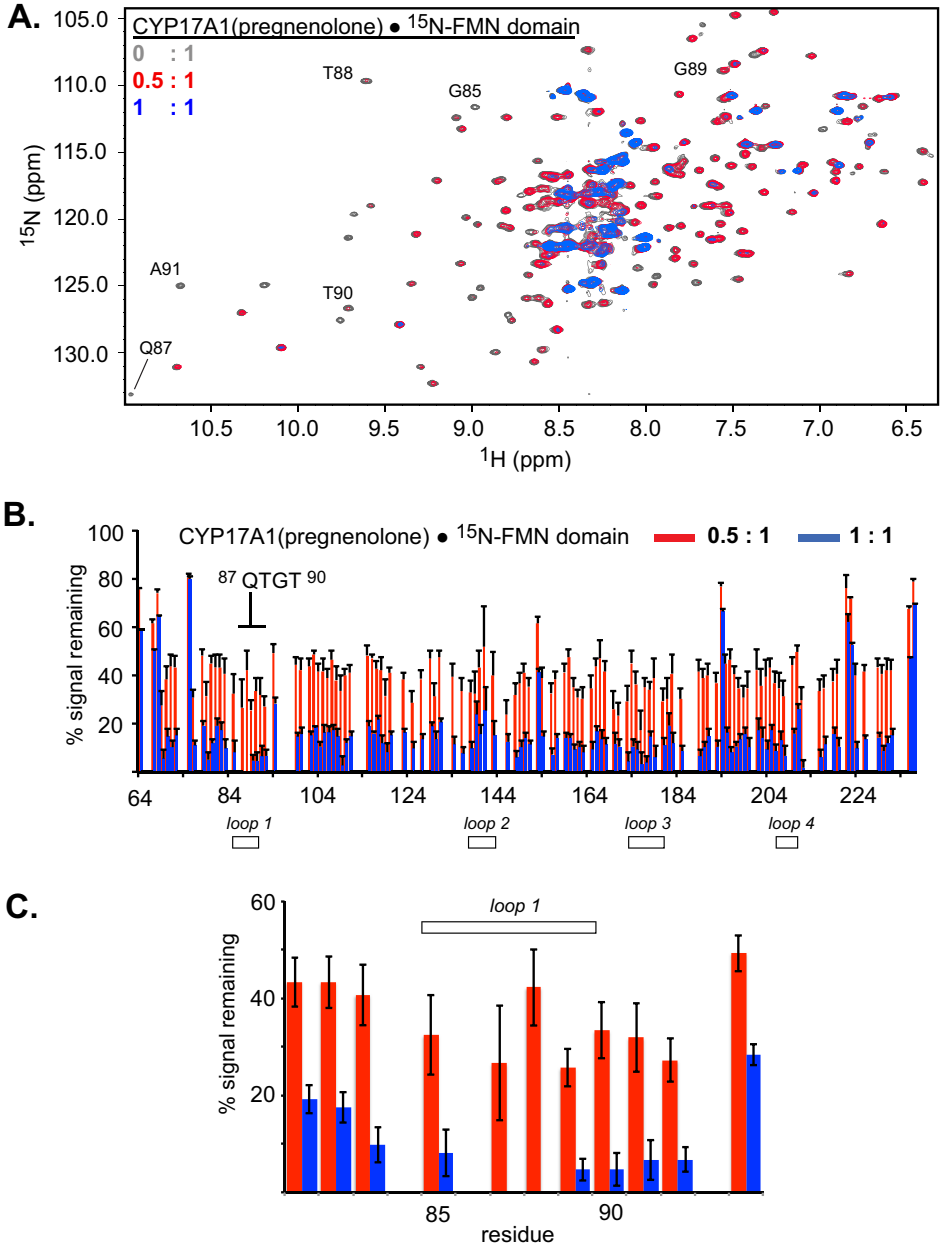

FIGURE 1. **Interaction of [^{15}N]FMN domain with CYP17A1.** *A,* stepwise addition of unlabeled CYP17A1(pregnenolone) induces differential line broadening effects on the ^{1}H-^{15}N HSQC spectrum of the FMN domain. *B,* plot of remaining signal intensities for a half-molar and a full molar equivalent of CYP17A1(pregnenolone) addition shows a modestly differential effect in residues 87–90 of loop 1. Gaps in this and following histograms indicate that a residue is not assigned, and thus data are not available at that position. *C,* close-up view of the differential effects observed in loop 1.

Formation of the CYP17A1·[^{15}N]FMN Complex Reveals More Extensive and More Uniform Line Broadening Than the Corresponding CYP17A1·[^{15}N]b_5 Complex—Interactions between the CPR FMN domain and CYP17A1 were first probed by generating the [^{15}N]FMN domain protein, adding unlabeled CYP17A1 at various stoichiometries and observing changes in the resulting [^{15}N]FMN domain HSQC spectra at 25 °C. As expected, the initial two-dimensional ^{1}H^{15}N HSQC spectrum of the 21.5-kDa FMN domain alone (Fig. 1*A*, 0:1 in *dark gray*) is relatively well dispersed. Chemical shift assignments had been previously reported for a very similar construct (7, 29) (BMRB entry 9301). Using the previous data, ~75% of the resonances could be unambiguously assigned in the current [^{15}N]FMN domain spectra. Upon addition of increasing concentrations of unlabeled CYP17A1, chemical shift perturbations of the FMN domain are negligible (Fig. 1*A*). Instead the spectrum of the [^{15}N]FMN domain undergoes considerable and progressive line broadening (CYP17A1(pregnenolone)·[^{15}N]FMN shown in Fig. 1*A* in *red* for 0.5:1 and in *blue* for 1:1 spectra, with signal intensities quantitated in Fig. 1*B*). Such line broadening is consistent with an interaction between CYP17A1 and [^{15}N]FMN occurring in the intermediate exchange time regime. Line broadening is decreased in the presence of a higher ionic strength buffer (75 mM NaCl *versus* 50 mM NaCl, data not shown), consistent with previous observations that the interaction between the FMN domain

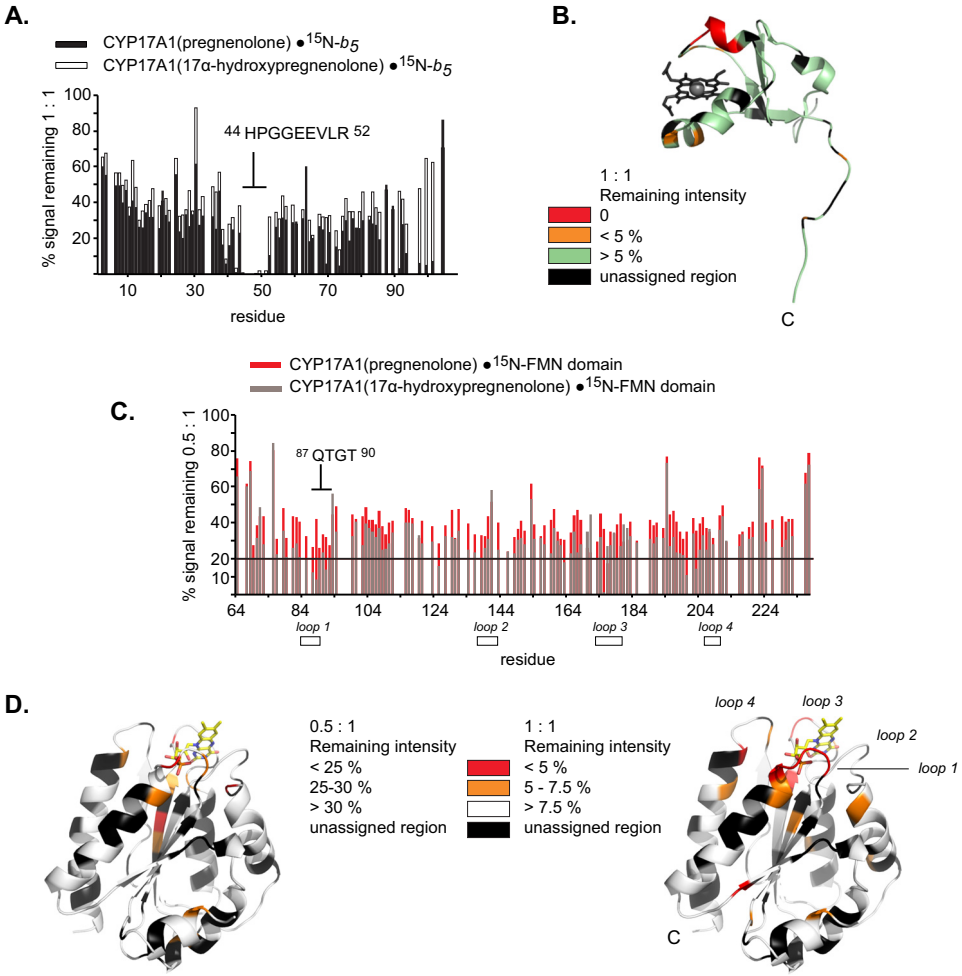

FIGURE 2. **Comparison of line broadening effects for [^{15}N]b_5 or [^{15}N]FMN titrated with CYP17A1.** *A*, [^{15}N]b_5 titrated with CYP17A1 saturated with either pregnenolone or 17α-hydroxypregnenolone demonstrates differential line broadening in a region that maps onto helix 2 in b_5, as shown in *B*. In contrast, the [^{15}N]FMN domain titration with CYP17A1 saturated with either ligand reveals more uniform line broadening but with moderately more substantial effects for certain residues at either 0.5:1 (*C*) or 1:1 (Fig. 1, *B* and *C*). *D*, mapping the most affected regions in CYP17A1(pregnenolone) at either 0.5:1 (*left panel*) or 1:1 (*right panel*) shows the most effects in or near loop 1 of the FMN binding pocket (Protein Data Bank code 1B1C) (26). Because the line broadening is progressive, different cutoffs are used (as shown in the legend) to highlight the most significant changes at each ratio. Part of the data in *A* is shown for comparison purposes and was originally published by Scott and co-workers (23).

and P450 enzymes are largely mediated by electrostatics (5, 41).

Comparisons reveal substantial differences between the line broadening observed herein for formation of the CYP17A1·[^{15}N]FMN complex and parallel titrations to form CYP17A1·[^{15}N]b_5 complexes (23). First, addition of CYP17A1 to [^{15}N]FMN domain results in much more extensive line broadening than CYP17A1 addition to [^{15}N]b_5. Addition of CYP17A1 to the [^{15}N]FMN domain at 1:1 results in retention of only ~10–20% of the original signal for most [^{15}N]FMN resonances (Fig. 1*B*, *blue 1:1 bars*). In contrast, addition of CYP17A1 to [^{15}N]b_5 at a 1:1 molar ratio resulted in the retention of ~40% of the original signals for [^{15}N]b_5 (Fig. 2*A*). A second difference is that line broadening upon formation of the CYP17A1·[^{15}N]FMN complex is much more uniform across the protein (Fig. 1*B*), whereas formation of the CYP17A1·[^{15}N]b_5 complex produces line broadening that is much more substantial for b_5 residues in the vicinity of Glu-48 and Glu-49 (Fig. 2*A*), which includes an anionic surface of b_5 (Fig. 2*B*). Although both interactions fall broadly in the intermediate time regime, these differences are consistent with an interaction between CYP17A1 and [^{15}N]b_5 that is further toward the fast end of the intermediate exchange regime than the interaction between CYP17A1 and [^{15}N]FMN. This is consistent with a stronger association between CYP17A1 and the CPR FMN domain than between CYP17A1 and b_5 and is consistent with a stronger interaction in general as reported between CPR and several xenobiotic metabolizing P450 enzymes (42).

Effect of Substrate on Formation of the CYP17A1·[^{15}N]FMN Domain Complex—The above experiments were accomplished with CYP17A1 saturated with its hydroxylase substrate pregnenolone. However, CYP17A1 can also convert the resulting 17α-hydroxypregnenolone product into dehydroepiandrosterone via an unusual lyase reaction. The two different substrates were previously found to modulate the CYP17A1 conformation (18) and CYP17A1·[^{15}N]b_5 interaction differently (23). Therefore, the interactions between CYP17A1 and [^{15}N]FMN were also evaluated in the presence of each substrate. Binding of CYP17A1 saturated with either substrate gen-

erally resulted in similar effects on the spectrum of the [^{15}N]FMN domain, but 17α-hydroxypregnenolone consistently promotes more extensive line broadening than when CYP17A1 is saturated with pregnenolone (0.5:1 titration point shown in Fig. 2*C*, *red pregnenolone bars versus gray 17α-hydroxypregnenolone bars*). This substrate dependence is suggestive of a stronger association between CYP17A1 and the FMN domain with the 17,20-lyase substrate present than with the hydroxylase substrate present. Intriguingly, the corresponding experiments examining substrate dependence of the CYP17A1·[^{15}N]b_5 complex revealed the opposite relationship, the CYP17A1(pregnenolone)·[^{15}N]b_5 complex was stronger (demonstrated more extensive line broadening) than the CYP17A1(17α-hydroxypregnenolone)·[^{15}N]b_5 complex (Fig. 2*A*) (23). These inverse outcomes suggest that substrates modulate *both* the CYP17A1·b_5 and CYP17A1·FMN domain complexes and in such a way that the effect may be cumulative.

Mapping Differential Line Broadening of the FMN Domain—Although the amount of line broadening was different for [^{15}N]FMN domain binding to CYP17A1 saturated with different substrates consistent with different affinities, the patterns of broadening were very similar, consistent with a conserved CYP17A1·[^{15}N]FMN domain interface. The sequential [^{15}N]FMN residues whose intensities were moderately but reproducibly reduced the most are ^{87}QTGT^{90}. For example, in the 1:1 CYP17A1(pregnenolone)·[^{15}N]FMN complex, these four residues retain less than 5% of their original intensity (Fig. 1, *B* and *C*). Similarly, at 0.5:1 residues 87–90 have some of the most substantial reductions in intensity (Fig. 2*C*). Other similarly affected but sequentially distributed residues include Gly-109, Leu-212, Leu-173, Lys-177, and Thr-178. When [^{15}N]FMN resonances with the most significant line broadening are mapped onto the structure of the FMN domain, the overall pattern is broadly similar at either the 0.5:1 or 1:1 molar ratios (Fig. 2*D*, *left panel versus right panel*). Although the progressive overall line broadening means the same absolute scale cannot be used for both ratios, it is clear that the most affected residues are primarily located on the surface of the FMN domain where the flavin mononucleotide cofactor is bound and where the interaction with CYP17A1 is expected to occur (Fig. 2*D*). Residues ^{87}QTGT^{90} form loop 1, one of four loops flanking the cofactor. Although residues Gln-87, Thr-88, and Thr-90 are completely conserved across species (43), they are not directly implicated in cofactor binding like those in loops 2 and 3. Instead loop 1 and the adjacent helix B demonstrate some small structural differences when the FMN domain is interacting with the CPR FAD domain compared to when the FMN domain is not associated with the FAD domain and presumably available for interaction with CYP17A1 (3, 5, 7). Of the other affected residues, Leu-212 and Leu-173 are located at the base of loops 3 and 4, respectively, with side chains that are oriented toward the interior of the FMN-binding site, at least in the crystal structure. The loop 3 residues Lys-177 and Thr-178 (also affected) appear solvent-exposed. Thus, the current NMR data suggest that residues near the flavin mononucleotide cofactor, including loop 1 region, are modulated by CYP17A1 binding and form part of the CYP17A1·[^{15}N]FMN domain interface regardless of the substrate in the CYP17A1 active site. At the higher 35 °C temperature, the specific effect on the broadening residues in the vicinity of loop 1 was slightly reduced (data not shown), which could be due to decreased affinity or changes in dynamics for the FMN domain.

Formation of the [^{15}N]CYP17A1·FMN Complex—Thus far, the focus of these experiments has been on probing and comparing CYP17A1·FMN and CYP17A1·b_5 interactions by observing changes in the spectra of [^{15}N]FMN and [^{15}N]b_5, respectively. To evaluate the effects of complex formation by monitoring the P450 protein directly, [^{15}N]CYP17A1 saturated with the inhibitor abiraterone was titrated with unlabeled FMN domain. Analysis of these spectra is made possible by two elements. First, we took advantage of our ongoing efforts to assign strategic NMR resonances for the 55-kDa CYP17A1. Select NMR assignments for CYP17A1 were initially generated by mutagenesis and selective labeling approaches (24). More recently, additional backbone assignments have been made using acquisition and analysis of triple resonance TRHNCA, TRHNCACB, TRHNCACO, and N-NOESY spectra. This ongoing assignment process has yielded assignments for residues that are well distributed in the CYP17A1 structure. Second, the use of abiraterone as the CYP17A1 ligand reduces the paramagnetic effect because this inhibitor forms a strong coordinate covalent bond with the heme iron, locking CYP17A1 into a low spin state. Using the combination, we have generated a set of assigned resonances, some of which are well resolved even in two-dimensional [^{1}H,^{15}N]CYP17A1 NMR spectra and can be used to monitor changes in [^{15}N]CYP17A1 (Fig. 3, *A*, listed below the *bars,* and *B*, regions shown in *blue*).

Stepwise titration of [^{15}N]CYP17A1 with the unlabeled FMN domain was optimized at 35 °C and primarily induced considerable and progressive line broadening of the [^{15}N]CYP17A1 (intensities for well resolved, assigned resonances shown in Fig. 3*A*). This is broadly consistent with the observation of the CYP17A1·FMN complex via the NMR spectra of the [^{15}N]FMN domain. However, although the line broadening observed for [^{15}N]FMN was largely uniform outside of the FMN domain loop 1 and other residues near the flavin mononucleotide binding region, the distribution of line broadening for [^{15}N]CYP17A1 was much less uniform and more extensive in specific regions (Fig. 3*A*, indicated with *arrows* for residues retaining less than 5% of their original intensity by the 1:0.5 titration point). Mapping of these residues onto the CYP17A1(abiraterone) structure reveals a clustered distribution lining the roof and borders of the active site (Fig. 3*C*). The assigned [^{15}N]CYP17A1 resonance most dramatically affected by titration with unlabeled FMN domain is Leu-102. Addition of only 0.25 molar eq of FMN reduced this resonance intensity to less than 10%, and by 1:0.35, no signal remains (Fig. 3*A*). Line broadening for adjacent residues Asp-103 and Ile-104 are also significant, with $<$5% remaining by 1:0.5 (Fig. 3*A*). Thus, all three of the resonances representing the B′-helix are obliterated or almost entirely broadened by 1:0.5. The CPR FMN domain is well established to bind by interacting with positively charged residues on the proximal face of other P450 enzymes (13), a binding site that in CYP17A1 is thought to partially overlap with the b_5-binding site (Fig. 3*B*) (23). Thus, binding of the FMN domain on the proximal side of the heme significantly

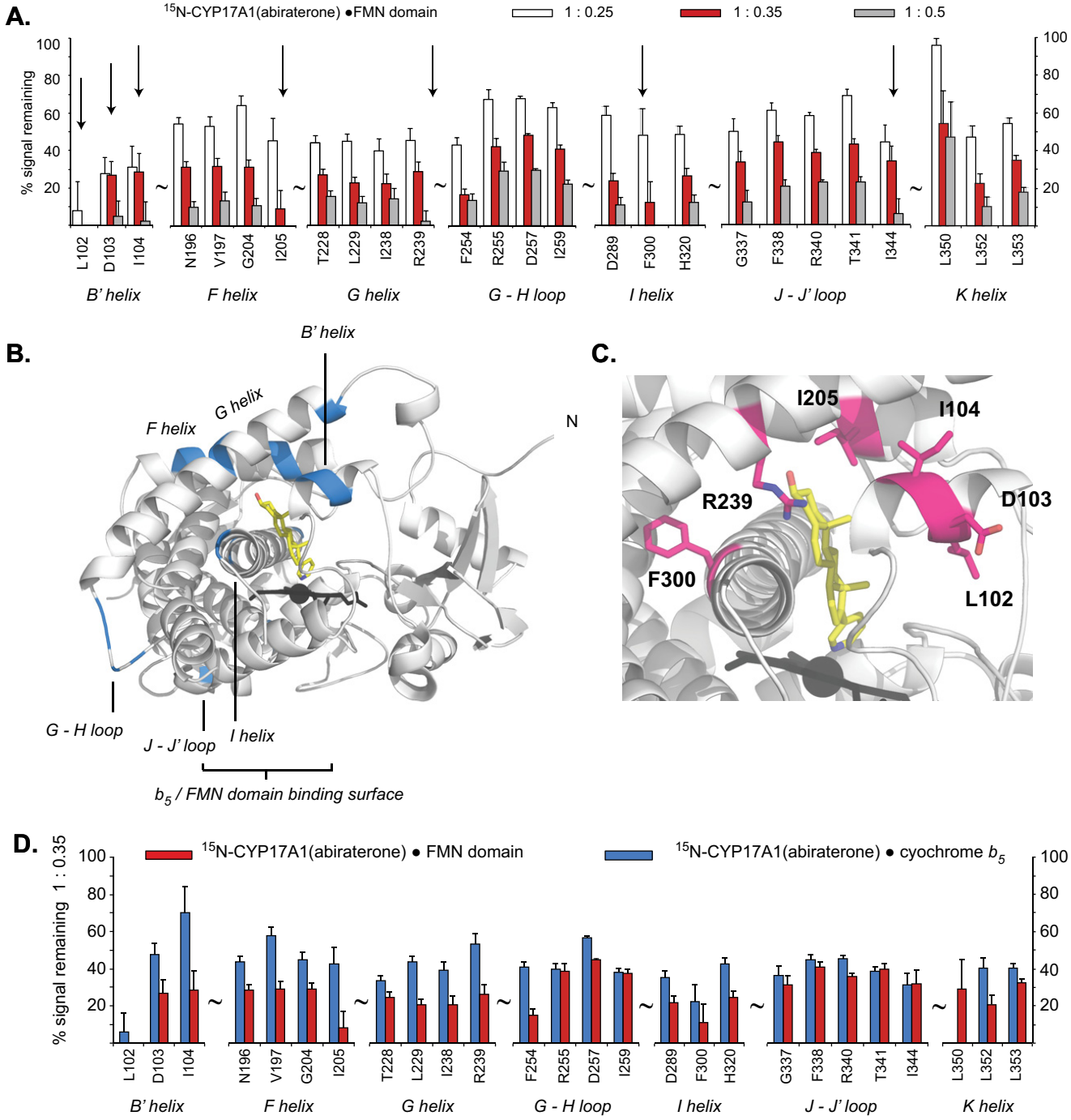

FIGURE 3. **Interaction of [^{15}N]CYP17A1(abiraterone) with the FMN domain.** *A,* stepwise addition of unlabeled FMN domain induces a pattern of differential line broadening in the CYP17A1 ^{1}H-^{15}N TROSY HSQC spectrum. Residues are shown in clusters representative of distinct CYP17A1 features, which are highlighted in *blue* in *B* (Protein Data Bank code 3RUK) (31). *C,* more pronounced peak broadening effects occur in specific residues adjacent to or bordering the distal end of the active site (also indicated as *arrows* in *A*. *D,* comparison of corresponding titration points (0.35 molar equivalent) of either FMN domain (*red*) or b_5 (*blue*) shows a general pattern of increased relative peak broadening for the CYP17A1, FMN domain complex.

influences the exchange dynamics of the B′-helix located ~45 Å away (Fig. 3*B*). Although the resonance for the adjacent B′ residue Ala-105 is not resolvable in the current experiments, mutation of Ala-105 to Leu is known to alter the regioselectivity of the hydroxylation reaction (44), influencing substrate orientation and enhancing substrate affinity, likely via alterations in the dynamics of this short helix (25). The B′-helix is generally considered one of the more flexible elements of P450 structure in general, with relatively few interactions between this short helix and the rest of the structure. The B′-helix can adopt different conformations with different ligands and is often thought to be involved in substrate access into the otherwise buried active site.

The next two resonances most substantially affected by FMN domain binding are those for Ile-205 and Phe-300. Both are completely broadened by 1:0.5 and have only ~10% signal remaining at 1:0.35 (Fig. 3*A*). In these cases, the changes in dynamics appear to be relatively specific as residues on either

side of Phe-300 and N-terminal to Ile-205 are much less affected. Both Ile-205 and Phe-300 occur in significant places in CYP17A1. The F-helix residue Ile-205 is directly adjacent to steroidal ligands with its side chain oriented inward toward the active site cavity (Fig. 3*C*) (25, 31). Importantly, Ile-205 is one helical turn from Asn-202. The side chains of Ile-205 and Asn-202 flank the A-ring of steroid substrates and the Asn-202 side chain hydrogen bonds with the three substituents of steroidal inhibitors or substrates (25, 31). Thus FMN domain binding alters the dynamics of another residue implicated in ligand binding. Residue Phe-300 is in the center of the I-helix that spans the P450 structure and crosses just above the heme, forming one "wall" of the active site, against which the steroid core packs (Fig. 3*C*). Phe-300 is on the opposite side of the I-helix facing away from ligands but is part of a turn of the I-helix with disruption of the normal backbone $i \rightarrow i + 4$ hydrogen bonding pattern. This is often the origin of either a break in the I-helix, which can allow the N-terminal half of the I-helix to bend away from its original axis, or a "bulge" of this region of the I-helix over the heme (45, 46).

An additional [^{15}N]CYP17A1 resonance that is substantially broadened upon FMN addition is that of residue Arg-239, with less than 5% signal remaining at 1:0.5 (Fig. 3*A*). Like Phe-300 and Ile-205, the effect seems to be relatively selective with much less line broadening for residues just N-terminal of Arg-239 (Fig. 3*A*). Once again, this residue is intimately associated with ligand binding, projecting from the G-helix into the active site and toward the steroid between the A- and B-rings (Fig. 3*C*).

Current limitations in the availability of NMR assignments for [^{15}N]CYP17A1 mean this represents only a partial mapping of line broadening effects upon binding of FMN. However, these observations suggest a link between FMN binding on the proximal surface of CYP17A1 and changes in the chemical exchange rate for regions of the protein implicated in substrate access and ligand binding. Notably, these changes are more significant than most of those in the J-J′ loop, which is actually closer to the actual FMN-binding site.

Several key differences are apparent upon comparison of changes in [^{15}N]CYP17A1 resonances when binding the FMN domain or when binding b_5. First, the interaction of [^{15}N]CYP17A1 with b_5 resulted in significant changes in resonance peak shape and redistributions between major and minor conformations for individual backbone signals in the F-, G-, and I-helices (24) (assignments were not available in B′ at the time). This type of change was distinctly not observed for the same [^{15}N]CYP17A1 resonances upon interaction with the FMN domain, as only peak broadening was observed. This comparison strongly supports the previously established biological role of b_5 as an allosteric modulator of CYP17A1 lyase activity (14, 15) by driving conformational selection of CYP17A1 (24). Binding of the FMN domain, and by extension possibly the entire CPR, does not alter CYP17A1 structure in this way.

Because the region between the F- and G-helices conformationally modulated by b_5 but not FMN is thought to modulate ligand entry, an orthogonal method was used to further probe this idea. Spectral titration of CYP17A1 with pregnenolone or 17α-hydroxypregnenolone was accomplished in the absence of partner proteins, in the presence of the isolated FMN domain or in the presence of b_5. Although an equimolar concentration of the FMN domain did not significantly alter the K_d values for either substrate, the presence of an equimolar concentration of b_5 reduced the K_d to ~55% of its original value for both substrates (data not shown). This supports the concept that b_5 alters the CYP17A1 conformation in such a way as to increase the affinity for both substrates.

A second difference between FMN and b_5 interactions with CYP17A1 is the degree of peak broadening observed for these two interactions. The intensities of [^{15}N]CYP17A1 resonances are generally reduced more upon binding the FMN domain than b_5 (example of [^{15}N]CYP17A1·b_5 or [^{15}N]CYP17A1·FMN domain at 1:0.35, Fig. 3*D*). This is consistent with a stronger CYP17A1·FMN interaction than the CYP17A1·b_5 interaction and is in agreement with the smaller dissociation constants reported for P450·CPR interactions (42). Similarly, FMN domain binding has a more significant effect than b_5 binding on line broadening of CYP17A1 residues, especially in the B′-helix (Ile-104 and Asp-103), the F-helix (especially Ile-205), the G-helix (especially Arg-239), one residue in the GH loop (Phe-254), and one residue in the K-helix (Leu-352). Conversely, Leu-350 in the K-helix is the only residue where b_5 has a more significant effect than the FMN domain (see below). Notably, these differential effects do not represent global structural changes, as intensities in the J-J′ loop are very similar for each interaction. Therefore, it is possible that different exchange dynamics related to either b_5 or the FMN domain binding to the proximal surface could uniquely impact ligand binding, orientation, or dissociation.

Distinctions between the CYP17A1·FMN and CYP17A1·b_5 Interactions—Although it is widely accepted that both b_5 and CPR bind via charge pairing interactions with the cationic proximal surface of P450 enzymes (12, 13, 23, 47), less is understood regarding the competitive or overlapping nature of these interactions. Partially overlapping b_5 and FMN-binding sites have been proposed on the proximal face of CYP2B4, leading to competitive binding (20). A recent NMR study demonstrated that [^{15}N]b_5 was released from the CYP17A1·[^{15}N]b_5 complex when CPR was added, consistent with a competitive interaction (23), but the degree of the binding site overlap is unknown.

The proximal CYP17A1 residues Arg-347, Arg-358, and Arg-449 (Fig. 4*A*) are thought to be involved in b_5 binding because of the following: 1) mutation of these residues to eliminate their charge obliterates the lyase reaction (requiring CPR and b_5) without disrupting the hydroxylase reaction (requiring only CPR) (48), and 2) these residues are required for formation of the CYP17A1·[^{15}N]b_5 complex (23). Unfortunately, assignments for these three Arg residues are not yet available, but distinct features in the current data drew our attention to the assigned backbone amide resonances for Leu-350 and Ile-344 located on either side of Arg-347 (Fig. 4*A*). These [^{15}N]CYP17A1 resonances are well resolved in a dispersed region of the NMR spectrum (Fig. 4*B*, *dark gray spectra*).

When [^{15}N]CYP17A1 is titrated with 0.35 molar eq of the FMN domain, the Leu-350 amide signal splits into several resonances and is broadened (Fig. 4*B*, *top left*). In contrast, addition of the same amount of b_5 results in Leu-350 peak broadening beyond detection (Fig. 4*B*, *top right*). As noted previously,

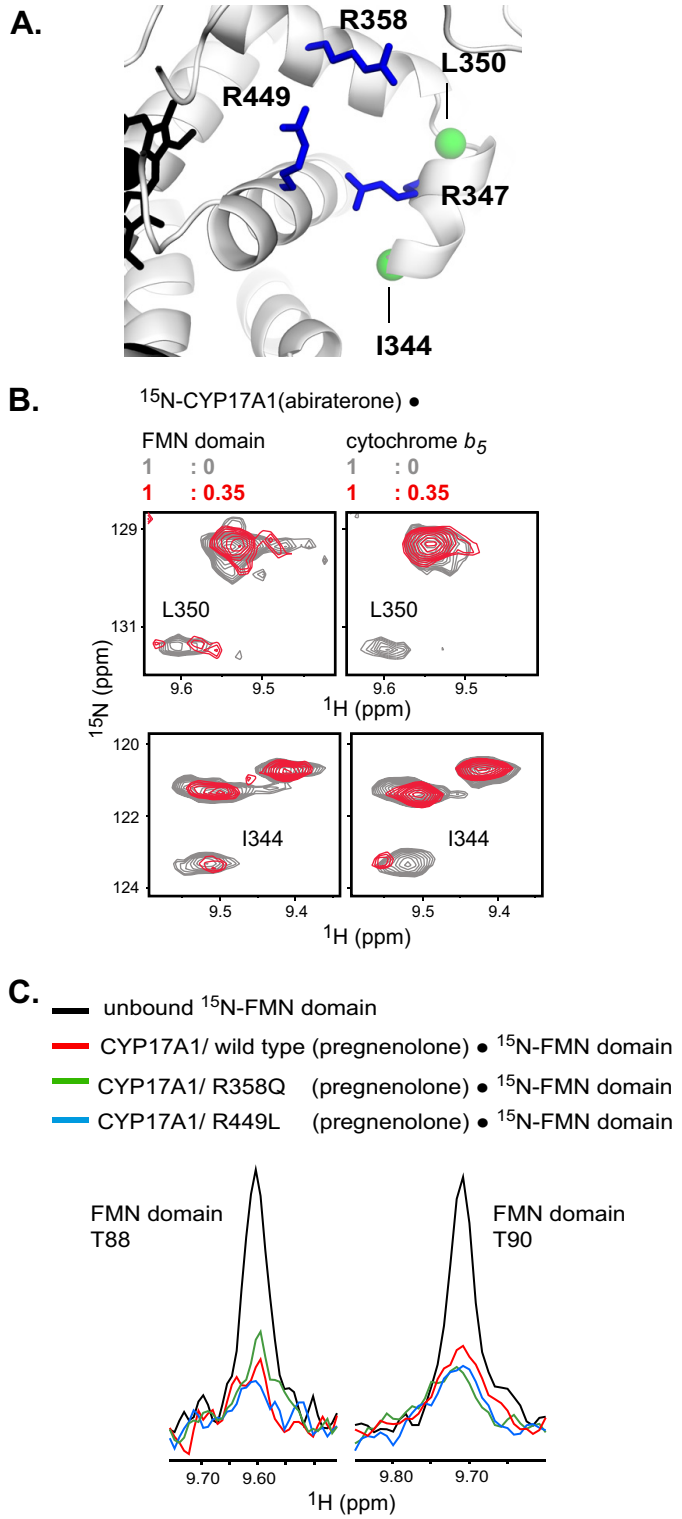

FIGURE 4. **Comparison of effects on the b_5 binding interface.** *A*, residues Arg-358, Arg-347, and Arg-449 of the proximal CYP17A1 surface are required to bind b_5 (23). *B*, monitoring the ^{1}H-^{15}N TROSY HSQC chemical shift values for Leu-350 and Ile-344, assignments near this cationic surface, shows that FMN or b_5 differentially affect this surface. *C*, pregnenolone-bound mutants R358Q and R449L do not disrupt the complex with the FMN domain, as read by the [^{15}N]FMN domain ^{1}H-^{15}N HSQC, underscoring the differences in the binding interfaces.

Leu-350 is the only assigned CYP17A1 residue more substantially affected by binding of b_5 than by binding of the FMN domain (Fig. 3*D*). Previous results revealed that [^{15}N]b_5 residues responsible for interacting with CYP17A1 experienced the greatest amount of line broadening (23). Similarly, extensive broadening of Leu-350 in the current [^{15}N]CYP17A1·b_5 experiment is consistent with CYP17A1 residue Leu-350 forming part of the [^{15}N]CYP17A1·b_5 interface. The fact that the [^{15}N]CYP17A1·FMN spectrum retains signal for Leu-350, albeit diminished, suggests that Leu-350 has dynamics that are distinct for these two different protein/protein interactions.

On the other side of Arg-347, the Ile-344 amide signal also shows distinct effects for both binding partners. Although binding of either FMN domain or b_5 to [^{15}N]CYP17A1 results in line broadening, FMN domain does not cause a significant change in chemical shift (Fig. 4*B*, *bottom left*), whereas b_5 addition shifts the resonance downfield (Fig. 4*B*, *bottom right*).

To further understand individual residue contributions to the two different CYP17A1/protein complexes, we employed mutagenesis in concert with NMR. The single-point CYP17A1 mutants R358Q or R449L prevent [^{15}N]b_5 binding to CYP17A1 (23). As discussed above, formation of the wild type CYP17A1(pregnenolone)·[^{15}N]FMN complex resulted in line broadening for FMN domain loop 1 residues, including Thr-88 and Thr-90 (one-dimensional spectra in Fig. 4*C*, *black versus red*). Substitution of the CYP17A1/R358Q or CYP17A1/R449L mutants for wild type CYP17A1 revealed similar line broadening (Fig. 4*C*, *green* and *blue*), indicating that the mutated CYP17A1 proteins still form a complex with the [^{15}N]FMN domain. Thus, the CYP17A1 mutations R358Q and R449L disrupt b_5 binding without adversely affecting binding of the FMN domain. This is consistent with these two mutations preventing the lyase reaction without impacting the hydroxylase reaction (48). Whether Arg-358 and Arg-449 on the CYP17A1 proximal surface are located outside of the FMN domain interface or whether a single substitution is simply insufficient to disrupt the stronger CYP17A1·[^{15}N]FMN interaction is unclear. Regardless, these observations highlight significant differences between the CYP17A1·b_5 complex and the CYP17A1·FMN domain complex that correlate with catalytically relevant functional differences.

Detection of a Weak Interaction between b_5 and the FMN Domain—Based on the hypothesis that formation of either complex is mutually competitive and previous data demonstrating that addition of CPR disrupted the CYP17A1·[^{15}N]b_5 complex (23), it was anticipated that the reverse would also be true; the addition of excess b_5 would disrupt the CYP17A1·FMN domain complex. To investigate this idea, CYP17A1 and [^{15}N]FMN were mixed in a 0.5:1 molar ratio so that [^{15}N]FMN was in excess. The CYP17A1 (pregnenolone)·[^{15}N]FMN complex was formed with typical line broadening of [^{15}N]FMN resonances (Fig. 5, *black versus red*). Then increasing amounts of unlabeled b_5 were added (Fig. 5, *blue* and *green*). If b_5 displaced [^{15}N]FMN domain from CYP17A1, the peak broadening of [^{15}N]FMN should be reversed, and the spectra should increasingly resemble that of the *top panel* in Fig. 5 (*black*). Instead, [^{15}N]FMN peaks continue to broaden until most of the signals in the dispersed regions of the spectrum of the FMN domain are undetectable by 0.5:1:3. This result can be interpreted in three different ways as follows: 1) formation of a trimeric complex; 2) enhancement of the CYP17A1·FMN

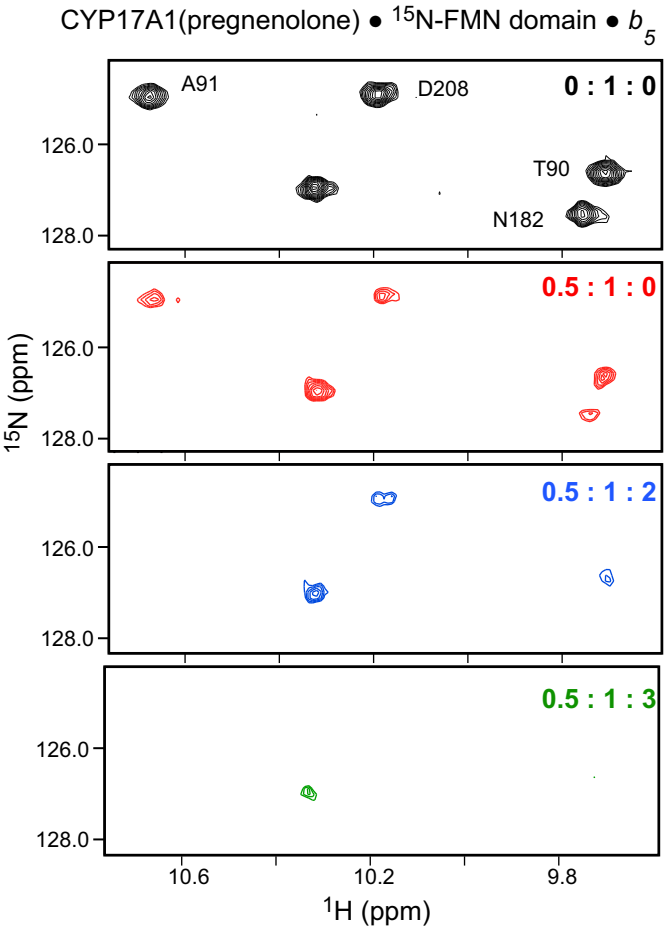

FIGURE 5. **Attempted disruption of the CYP17A1, FMN domain complex.** Stepwise addition of unlabeled b_5 (*blue* and *green* spectra for a 2- and 3-fold addition, respectively) enhances rather than lessens the peak broadening effects of the CYP17A1, FMN domain complex (*red* spectrum).

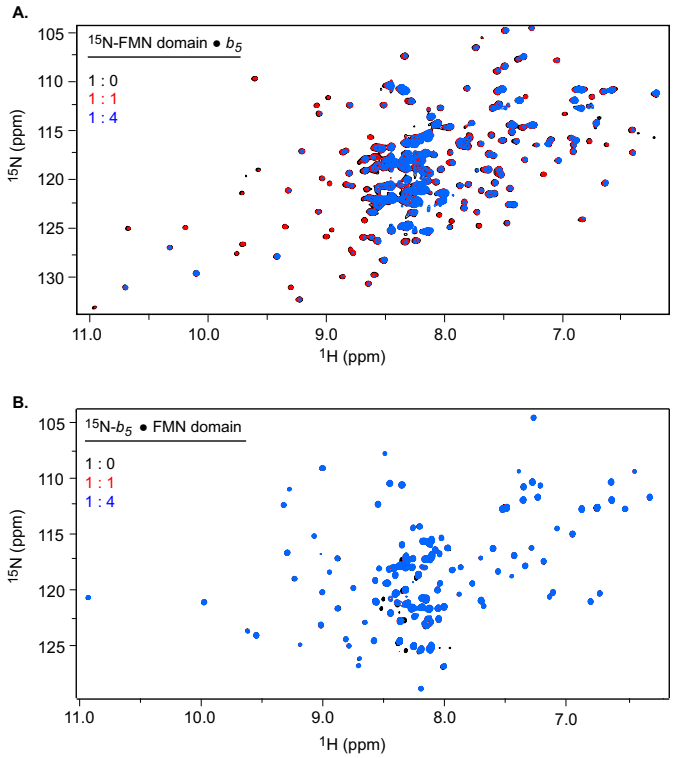

FIGURE 6. **^{1}H-^{15}N HSQC spectrum of the interaction of the FMN domain and b_5.** *A*, titration of [^{15}N]FMN with b_5 reveals line-broadening effects in the FMN domain, suggesting a weak interaction that requires a minimum of 2-fold unlabeled b_5. *B*, however, titration of [^{15}N]b_5 with FMN shows no peak broadening effects in b_5, suggesting the exchange dynamics of the interaction are very different for each protein.

domain complex in the presence of b_5; or 3) a direct interaction between b_5 and the FMN domain.

CPR is known to reduce b_5 (49, 50), and a weak interaction between b_5 and CPR has previously been detected (42). To understand the significance of interactions between FMN domain and b_5, titrations were completed with the ^{15}N isotopic label on either the FMN domain or b_5. In other words, [^{15}N]FMN was titrated with b_5 (Fig. 6*A*), and [^{15}N]b_5 was titrated with FMN domain (Fig. 6*B*).

When [^{15}N]FMN was titrated with b_5, line broadening was observed, with peak broadening first noticeable with addition of 2-fold b_5 and becoming substantial upon addition of 4-fold molar excess of b_5 (Fig. 6*A*). These data are consistent with the generation of a [^{15}N]FMN·b_5 complex, but the requirement for a 2–4-fold molar excess of b_5 in order to observe line broadening is substantially higher than the submolar ratios of b_5 or FMN domain that cause line broadening of [^{15}N]CYP17A1 or the line broadening of [^{15}N]FMN domain or [^{15}N]b_5 by CYP17A1. This suggests that the interaction between the FMN domain and b_5 is very weak relative to that between CYP17A1 and either protein.

The reverse titration of [^{15}N]b_5 with increasing concentrations of FMN domain did not induce similar peak broadening of the b_5 signal (Fig. 6*B*). The absence of peak broadening from the [^{15}N]b_5 perspective suggests that the exchange dynamics for the interaction are vastly different for each respective protein.

It is unclear whether such a weak interaction between b_5 and the FMN domain of CPR plays a role in the biological context of CYP17A1 enzyme function, but this interaction presented an unexpected variable in determining whether the FMN domain competes with b_5 for a binding surface on CYP17A1. The continued peak broadening observed for [^{15}N]FMN domain in the three-component system (Fig. 5) is likely due to this peripheral interaction of [^{15}N]FMN with b_5 at high concentrations of b_5.

Detection of a Competitive Interaction between b_5 and the FMN Domain for CYP17A1—To probe the nature of CYP17A1 interaction with both FMN and b_5 simultaneously without interference from weak binding between b_5 and the FMN domain, an alternative titration was designed taking advantage of the following: 1) the "silence" of [^{15}N]b_5 with respect to the weak FMN·b_5 interaction, and 2) the ability to monitor [^{15}N]b_5 resonances for Glu-48 and Glu-49, which are sensitive to CYP17A1·b_5 complex formation. Thus, a fixed, limiting amount of CYP17A1(substrate) (Fig. 7, *A* and *B*, *gray lines*) was mixed with a fixed excess amount of [^{15}N]b_5 so that all of the CYP17A1 would be sequestered in the resulting CYP17A1·[^{15}N]b_5 complex with substantial reduction in peak intensity due to line broadening (Fig. 7, *A* and *B*, *black lines*), as observed previously (23). Subsequent spectra containing increasing amounts of unlabeled FMN domain induce a marked and progressive recovery of the Glu-48 and Glu-49 resonances for the CYP17A1(17α-hydroxypregnenolone)·[^{15}N]b_5 complex (Fig.

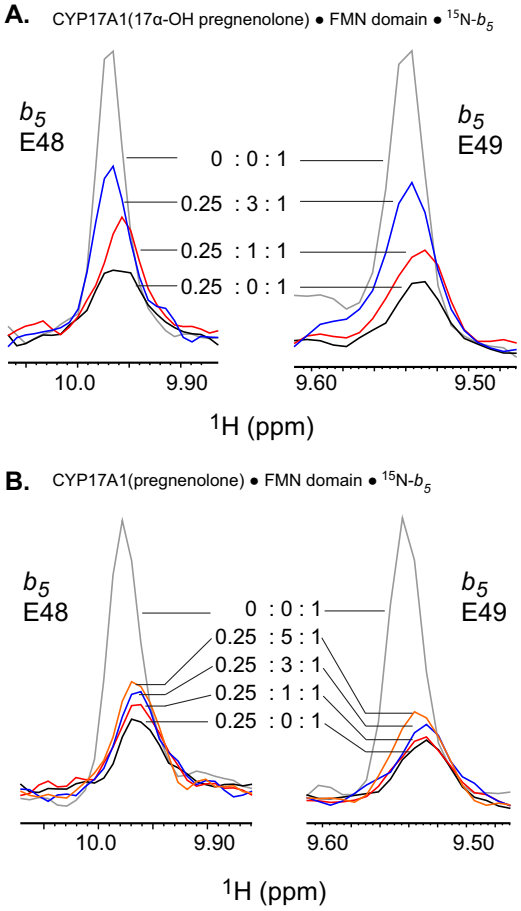

FIGURE 7. **Competition by the FMN domain of the CYP17A1, b_5 complex.** Monitoring the complex from the perspective of ^{1}H-^{15}N b_5, in which unlabeled FMN domain is titrated into different samples, reveals a gradual release of b_5 from the complex as reported by the most affected residues Glu-48 and Glu-49. The release of b_5 is noticeably more pronounced from the CYP17A1(17α-hydroxypregnenolone) complex (*A*) than for the pregnenolone-bound complex (*B*).

7*A*) and a smaller progressive recovery from the CYP17A1 (pregnenolone)·[^{15}N]b_5 (Fig. 7*B*) complex. Both the recovery of these specific [^{15}N]b_5 signals and the larger effect when the 17α-hydroxypregnenolone lyase substrate is bound are consistent with parallel experiments with intact CPR (23). In both cases the results suggest a competitive relationship in which binding of the CPR FMN domain to CYP17A1 results in displacement of b_5 and reinforce a role for specific substrates in modulating CYP17A1·b_5 and CYP17A1·CPR complexes.

Discussion

The precise mechanisms underlying the respective 17α-hydroxylase and 17,20-lyase activities of CYP17A1 have been enigmatic, but are of considerable interest to ongoing drug design efforts. This is because selective inhibition of 17,20-lyase activity is desirable to block androgen biosynthesis in the treatment of metastatic prostate cancer, but concomitant inhibition of the 17α-hydroxylase activity causes substantial clinical side effects (51). The only Food and Drug Administration-approved CYP17A1 inhibitor, abiraterone, inhibits both lyase and hydroxylase reactions and requires co-treatment with prednisone to mitigate mineralocorticoid excess from concurrent inhibition of the hydroxylase reaction (52). Because b_5 is not needed for the hydroxylation reaction but facilitates the lyase reaction, disruption of b_5 interaction is a logical goal, so long as CPR interactions are not compromised.

Integration of this new information probing CYP17A1 structure and protein/protein interactions with existing knowledge on the enzymatic function suggests a model for this complex system (Fig. 8). The first element to this model is an equilibrium between conformational states of CYP17A1 depending on ligand and b_5 interaction, represented by the hypothetical conformations "A" and "B" in Fig. 8. This concept is consistent with multiple lines of evidence. First, it is clear from x-ray structures with different substrates and inhibitors that there are at least two conformations of the region between the F- and G-helices (25, 31), regions that have been repeatedly associated with substrate access in multiple P450 enzymes (53, 54). In the x-ray structures, there are equal ratios of the two conformations, but this may be dictated by crystalline packing requirements and may not reflect the native distribution of conformational states. Second, previous NMR reports have established that when CYP17A1 is saturated with different substrates in solution the residues in the F- and G-helices are differently affected (24), supporting the concept that different substrates shift the equilibrium between distinct conformational states. Third, the population of conformational states is further influenced by addition of b_5 (24). Thus, binding of pregnenolone promotes a conformational state labeled here as state A, which would be capable of interaction with CPR to perform the hydroxylase reaction in a canonical P450 reaction cycle.

However, when 17α-hydroxypregnenolone is bound and b_5 is present, a progressive conversion to a different conformational state is known to occur (24), which is called the B state in Fig. 8. NMR and mutational studies have previously shown that the anionic b_5 residues Glu-48 and Glu-49 are essential for binding to CYP17A1, and CYP17A1 residues Arg-358 and Arg-449 are likewise essential for binding b_5 (23). Although b_5 binds to the proximal face of CYP17A1, several of the residues affected by this interaction are located on the opposite side of CYP17A1 in the F and G regions of the protein that interact with the membrane and are involved in substrate access. This suggests that the CYP17A1·b_5 interaction, which promotes the lyase reaction 10-fold, may do so by reinforcing this B conformation with an F/G structure that reduces dissociation of the lyase substrate. In addition to the structural data (24), an allosteric role for b_5 has long been postulated in P450 regulation (14, 55, 56). This is particularly true for CYP17A1 because either the apo- or holo-form of b_5 has been shown to enhance lyase activity 10-fold without electron transfer (15). The second element of this model is CYP17A1 interaction with b_5 *versus* CPR or the FMN domain. Because 1) CYP17A1 requires two electrons delivered by CPR in order for catalysis of the lyase reaction to occur and 2) CPR and b_5 are thought to have at least a partially overlapping binding site on the proximal CYP17A1 face (13, 20), the binding and electron delivery by CPR necessitates the release of b_5 (Fig. 8). As demonstrated by NMR, either CPR (23, 24) or its isolated FMN domain (Fig. 7) can indeed displace b_5. It is the latter interactions between the CPR FMN domain and CYP17A1 that are the primary focus of this work.

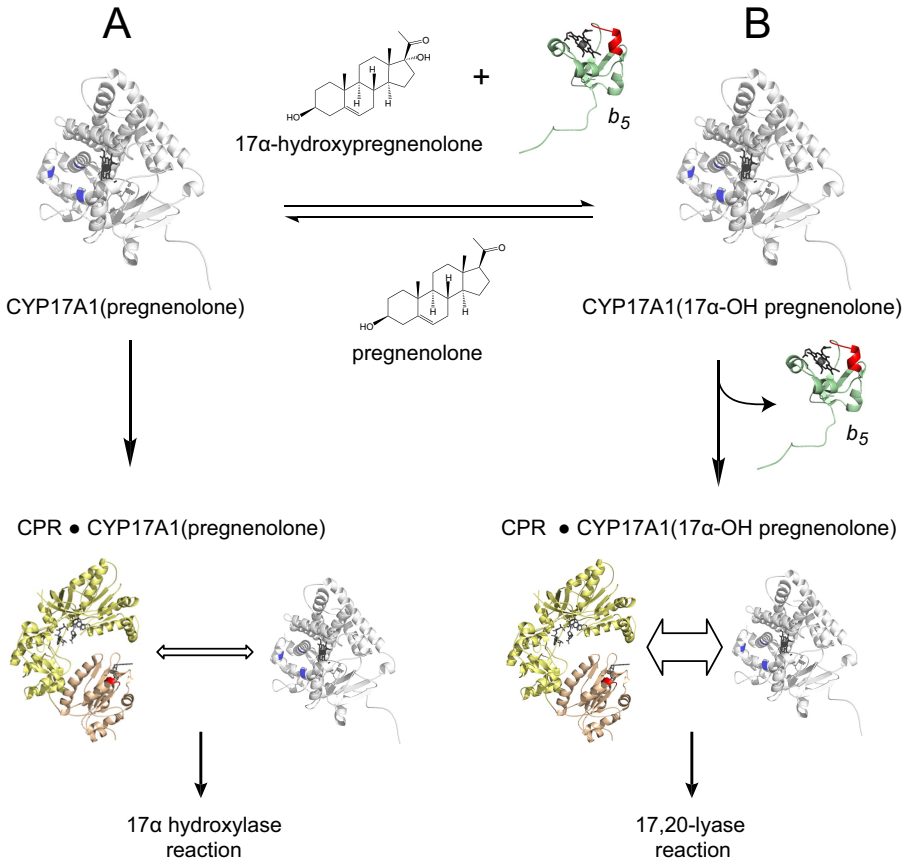

FIGURE 8. **NMR supported model of CYP17A1 regulation.** This and recent NMR studies support a two-step model of CYP17A1 regulation. First, turnover of hydroxylase substrate in combination with the effects of b_5 promote a redistribution of populated states as supported by Ref. 24. The hypothetical state B then results in a stronger association with CPR resulting in displacement of b_5. A stronger association with CPR (as reported by enhanced displacement of bound b_5) in the presence of lyase substrate is supported by this along with a previous study (23).

The isolated FMN domain, which has the same structure as in the full-length CPR enzyme (4–6) and which is active in electron transfer (27, 28), is used herein. Not surprisingly, the current NMR data implicate residues surrounding the flavin prosthetic group of the FMN domain in interactions with CYP17A1, because intensities for these residues show the most significant intensity reductions upon combination of the two proteins (Figs. 1*B* and 2*C*). The affinity for FMN domain binding to CYP17A1 appears to differ somewhat in the presence of different substrates (Fig. 2*C*). Herein, the 17α-hydroxypregnenolone-bound B state appears to associate more strongly with the FMN domain than the pregnenolone-bound A state (depicted by relative *arrow size* between CYP17A1 and CPR in Fig. 8). This result is consistent with similar results using CPR, where CPR displaced more b_5 from CYP17A1(17α-hydroxypregnenolone) than from CYP17A1(pregnenolone). This idea is also consistent with previous proposals for a stronger electron transfer complex during the b_5-modulated lyase reaction (14) and enhanced lyase activity observed in phosphorylated CYP17A1 (proposed to enhance its interaction with CPR) (57). Finally, reports that disrupted lyase activity resulting from mutations in the surface of CYP17A1 implicated in b_5 binding (R347H and R358Q) can be partially overcome by the presence of both b_5 and CPR together (58) and also suggest a b_5-related enhancement of the CYP17A1·CPR complex.

Further comparisons between CYP17A1 interactions with FMN domain and b_5 are consistent with the proposed model. The two binding partners have subtly different interactions with residues on the CYP17A1 proximal face, including Ile-344 and Leu-350 (Fig. 4*B*). This is further underscored by the fact that mutation of CYP17A1 proximal residues Arg-358 or Arg-449 each disrupt b_5 binding (23), but neither single mutation disrupts FMN domain binding (Fig. 4*D*). Although the FMN domain appears to bind to CYP17A1 with higher affinity than b_5 (Fig. 3*D*), the FMN domain does not appear to substantially alter the CYP17A1 conformation like b_5 does, as evidenced by the absence of peak splitting that was observed for interaction with b_5. Aside from one resonance in the J-J′ loop on the CYP17A1 proximal face, interaction with the FMN domain has the most significant effects on the resonances of residues lining the CYP17A1 active site (Fig. 3*A*) that may help promote subsequent steps in the catalytic cycle.

Notably, at no point has the NMR data using the soluble domains supported the presence of a trimeric complex. Although there is a detectable interaction between b_5 and the FMN domain, which may contribute to the reported ability of CPR to reduce b_5 directly *in vitro* (50), such an interaction appears to be very weak and may not be physiologically relevant.

In summary, the structural data herein provide a structural mechanism bridging both conventional hypotheses, in which

CYP17A1 regulation of the CYP17A1(17α-hydroxypregnenolone) lyase reaction is achieved first via a b_5-induced allosteric effect, followed in turn by a stronger association with CPR.

Author Contributions—D. F. E., J. S. L., and E. E. S. participated in research design; D. F. E. and E. E. S. conducted the experiments; D. F. E., J. S. L., and E. E. S. performed data analysis; and D. F. E., J. S. L., and E. E. S. wrote or contributed to the writing of the manuscript.

Acknowledgments—E. coli strain NCM533 was a gift from Tom Pochapsky at Brandeis University. NMR data were collected at the University of Kansas Biomolecular NMR Laboratory, supported in part by Center of Biomedical Research Excellence in Protein Structure and Function, National Institutes of Health Grants RR01778 and GM103420, or the Brandeis University Nuclear Magnetic Resonance Facility, with the assistance of Director Dr. Susan Sondej Pochapsky.

References

1. Shen, A. L., O'Leary, K. A., and Kasper, C. B. (2002) Association of multiple developmental defects and embryonic lethality with loss of microsomal NADPH-cytochrome P450 oxidoreductase. *J. Biol. Chem.* **277,** 6536–6541
2. Waskell, L., and Kim, J.-J. P. (2005) in *Cytochrome P450: Structure, Mechanism, and Biochemistry* (Ortiz de Montellano, P. R., ed) 4th Ed., pp. 33–68, Kluwer Academic/Plenum Publishers, New York
3. Xia, C., Panda, S. P., Marohnic, C. C., Martásek, P., Masters, B. S., and Kim, J. J. (2011) Structural basis for human NADPH-cytochrome P450 oxidoreductase deficiency. *Proc. Natl. Acad. Sci. U.S.A.* **108,** 13486–13491
4. Wang, M., Roberts, D. L., Paschke, R., Shea, T. M., Masters, B. S., and Kim, J. J. (1997) Three-dimensional structure of NADPH-cytochrome P450 reductase: Prototype for FMN- and FAD-containing enzymes. *Proc. Natl. Acad. Sci. U.S.A.* **94,** 8411–8416
5. Hamdane, D., Xia, C., Im, S. C., Zhang, H., Kim, J. J., and Waskell, L. (2009) Structure and function of an NADPH-cytochrome P450 oxidoreductase in an open conformation capable of reducing cytochrome P450. *J. Biol. Chem.* **284,** 11374–11384
6. Ellis, J., Gutierrez, A., Barsukov, I. L., Huang, W. C., Grossmann, J. G., and Roberts, G. C. (2009) Domain motion in cytochrome P450 reductase: Conformational equilibria revealed by NMR and small-angle x-ray scattering. *J. Biol. Chem.* **284,** 36628–36637
7. Huang, W. C., Ellis, J., Moody, P. C., Raven, E. L., and Roberts, G. C. (2013) Redox-linked domain movements in the catalytic cycle of cytochrome P450 reductase. *Structure* **21,** 1581–1589
8. Laursen, T., Jensen, K., and Møller, B. L. (2011) Conformational changes of the NADPH-dependent cytochrome P450 reductase in the course of electron transfer to cytochromes P450. *Biochim. Biophys. Acta* **1814,** 132–138
9. Iyanagi, T., Xia, C., and Kim, J. J. (2012) NADPH-cytochrome P450 oxidoreductase: Prototypic member of the diflavin reductase family. *Arch. Biochem. Biophys.* **528,** 72–89
10. Kenaan, C., Zhang, H., Shea, E. V., and Hollenberg, P. F. (2011) Uncovering the role of hydrophobic residues in cytochrome P450-cytochrome P450 reductase interactions. *Biochemistry* **50,** 3957–3967
11. Estabrook, R. W., Shet, M. S., Fisher, C. W., Jenkins, C. M., and Waterman, M. R. (1996) The interaction of NADPH-P450 reductase with P450: an electrochemical study of the role of the flavin mononucleotide-binding domain. *Arch. Biochem. Biophys.* **333,** 308–315
12. Bridges, A., Gruenke, L., Chang, Y. T., Vakser, I. A., Loew, G., and Waskell, L. (1998) Identification of the binding site on cytochrome P450 2B4 for cytochrome b_5 and cytochrome P450 reductase. *J. Biol. Chem.* **273,** 17036–17049
13. Im, S. C., and Waskell, L. (2011) The interaction of microsomal cytochrome P450 2B4 with its redox partners, cytochrome P450 reductase and cytochrome b_5. *Arch. Biochem. Biophys.* **507,** 144–153
14. Akhtar, M. K., Kelly, S. L., and Kaderbhai, M. A. (2005) Cytochrome b_5 modulation of 17α-hydroxylase and 17–20 lyase (CYP17) activities in steroidogenesis. *J. Endocrinol.* **187,** 267–274
15. Auchus, R. J., Lee, T. C., and Miller, W. L. (1998) Cytochrome b_5 augments the 17,20-lyase activity of human P450c17 without direct electron transfer. *J. Biol. Chem.* **273,** 3158–3165
16. Hall, P. F. (1991) Cytochrome P-450 C21scc: One enzyme with two actions: hydroxylase and lyase. *J. Steroid Biochem. Mol. Biol.* **40,** 527–532
17. Zhao, C., Gao, Q., Roberts, A. G., Shaffer, S. A., Doneanu, C. E., Xue, S., Goodlett, D. R., Nelson, S. D., and Atkins, W. M. (2012) Cross-linking mass spectrometry and mutagenesis confirm the functional importance of surface interactions between CYP3A4 and holo/apo cytochrome b_5. *Biochemistry* **51,** 9488–9500
18. Naffin-Olivos, J. L., and Auchus, R. J. (2006) Human cytochrome b_5 requires residues E48 and E49 to stimulate the 17,20-lyase activity of cytochrome P450c17. *Biochemistry* **45,** 755–762
19. Zhang, H., Hamdane, D., Im, S. C., and Waskell, L. (2008) Cytochrome b_5 inhibits electron transfer from NADPH-cytochrome P450 reductase to ferric cytochrome P450 2B4. *J. Biol. Chem.* **283,** 5217–5225
20. Zhang, H., Im, S. C., and Waskell, L. (2007) Cytochrome b_5 increases the rate of product formation by cytochrome P450 2B4 and competes with cytochrome P450 reductase for a binding site on cytochrome P450 2B4. *J. Biol. Chem.* **282,** 29766–29776
21. Tripathi, S., Li, H., and Poulos, T. L. (2013) Structural basis for effector control and redox partner recognition in cytochrome P450. *Science* **340,** 1227–1230
22. Ahuja, S., Jahr, N., Im, S. C., Vivekanandan, S., Popovych, N., Le Clair, S. V., Huang, R., Soong, R., Xu, J., Yamamoto, K., Nanga, R. P., Bridges, A., Waskell, L., and Ramamoorthy, A. (2013) A model of the membrane-bound cytochrome b_5-cytochrome P450 complex from NMR and mutagenesis data. *J. Biol. Chem.* **288,** 22080–22095
23. Estrada, D. F., Laurence, J. S., and Scott, E. E. (2013) Substrate-modulated cytochrome P450 17A1 and cytochrome b_5 interactions revealed by NMR. *J. Biol. Chem.* **288,** 17008–17018
24. Estrada, D. F., Skinner, A. L., Laurence, J. S., and Scott, E. E. (2014) Human cytochrome P450 17A1 conformational selection: modulation by ligand and cytochrome b_5. *J. Biol. Chem.* **289,** 14310–14320
25. Petrunak, E. M., DeVore, N. M., Porubsky, P. R., and Scott, E. E. (2014) Structures of human steroidogenic cytochrome P450 17A1 with substrates. *J. Biol. Chem.* **289,** 32952–32964
26. Zhao, Q., Modi, S., Smith, G., Paine, M., McDonagh, P. D., Wolf, C. R., Tew, D., Lian, L. Y., Roberts, G. C., and Driessen, H. P. (1999) Crystal structure of the FMN-binding domain of human cytochrome P450 reductase at 1.93 Å resolution. *Protein Sci.* **8,** 298–306
27. Smith, G. C., Tew, D. G., and Wolf, C. R. (1994) Dissection of NADPH-cytochrome P450 oxidoreductase into distinct functional domains. *Proc. Natl. Acad. Sci. U.S.A.* **91,** 8710–8714
28. Zhao, Q., Smith, G., Modi, S., Paine, M., Wolf, R. C., Tew, D., Lian, L. Y., Primrose, W. U., Roberts, G. C., and Driessen, H. P. (1996) Crystallization and preliminary x-ray diffraction studies of human cytochrome P450 reductase. *J. Struct. Biol.* **116,** 320–325
29. Barsukov, I., Modi, S., Lian, L. Y., Sze, K. H., Paine, M. J., Wolf, C. R., and Roberts, G. C. (1997) ^{1}H, ^{15}N and ^{13}C NMR resonance assignment, secondary structure and global fold of the FMN-binding domain of human cytochrome P450 reductase. *J. Biomol. NMR* **10,** 63–75
30. Mulrooney, S. B., and Waskell, L. (2000) High-level expression in *Escherichia coli* and purification of the membrane-bound form of cytochrome b_5. *Protein Expr. Purif.* **19,** 173–178
31. DeVore, N. M., and Scott, E. E. (2012) Structures of cytochrome P450 17A1 with prostate cancer drugs abiraterone and TOK-001. *Nature* **482,** 116–119
32. Delaglio, F., Grzesiek, S., Vuister, G. W., Zhu, G., Pfeifer, J., and Bax, A. (1995) NMRPipe: a multidimensional spectral processing system based on UNIX pipes. *J. Biomol. NMR* **6,** 277–293
33. Johnson, B. A. (2004) Using NMRView to visualize and analyze the NMR spectra of macromolecules. *Methods Mol. Biol.* **278,** 313–352
34. Vranken, W. F., Boucher, W., Stevens, T. J., Fogh, R. H., Pajon, A., Llinas, M., Ulrich, E. L., Markley, J. L., Ionides, J., and Laue, E. D. (2005) The

CCPN data model for NMR spectroscopy: development of a software pipeline. *Proteins* **59,** 687–696
35. Nunez, M., Guittet, E., Pompon, D., van Heijenoort, C., and Truan, G. (2010) NMR structure note: oxidized microsomal human cytochrome b_5. *J. Biomol. NMR* **47,** 289–295
36. Pervushin, K., Riek, R., Wider, G., and Wüthrich, K. (1997) Attenuated T2 relaxation by mutual cancellation of dipole-dipole coupling and chemical shift anisotropy indicates an avenue to NMR structures of very large biological macromolecules in solution. *Proc. Natl. Acad. Sci. U.S.A.* **94,** 12366–12371
37. Salzmann, M., Pervushin, K., Wider, G., Senn, H., and Wüthrich, K. (1998) TROSY in triple-resonance experiments: new perspectives for sequential NMR assignment of large proteins. *Proc. Natl. Acad. Sci. U.S.A.* **95,** 13585–13590
38. Salzman, M., Wider, G., Pervushin, K., Senn, H., and Wuthrich, K. (1999) TROSY-type triple-resonance experiments for sequential NMR assignments of large proteins. *J. Am. Chem. Soc.* **4,** 844–848
39. Sandee, D., and Miller, W. L. (2011) High-yield expression of a catalytically active membrane-bound protein: human P450 oxidoreductase. *Endocrinology* **152,** 2904–2908
40. Munro, A. W., Noble, M. A., Robledo, L., Daff, S. N., and Chapman, S. K. (2001) Determination of the redox properties of human NADPH-cytochrome P450 reductase. *Biochemistry* **40,** 1956–1963
41. Shen, A. L., and Kasper, C. B. (1995) Role of acidic residues in the interaction of NADPH-cytochrome P450 oxidoreductase with cytochrome P450 and cytochrome c. *J. Biol. Chem.* **270,** 27475–27480
42. Shimada, T., Mernaugh, R. L., and Guengerich, F. P. (2005) Interactions of mammalian cytochrome P450, NADPH-cytochrome P450 reductase, and cytochrome b_5 enzymes. *Arch. Biochem. Biophys.* **435,** 207–216
43. Pandey, A. V., and Flück, C. E. (2013) NADPH P450 oxidoreductase: structure, function, and pathology of diseases. *Pharmacol. Ther.* **138,** 229–254
44. Swart, A. C., Storbeck, K. H., and Swart, P. (2010) A single amino acid residue, Ala 105, confers 16α-hydroxylase activity to human cytochrome P450 17α-hydroxylase/17,20 lyase. *J. Steroid Biochem. Mol. Biol.* **119,** 112–120
45. Poulos, T. L. (2003) Cytochrome P450 flexibility. *Proc. Natl. Acad. Sci. U.S.A.* **100,** 13121–13122
46. Gay, S. C., Roberts, A. G., and Halpert, J. R. (2010) Structural features of cytochromes P450 and ligands that affect drug metabolism as revealed by x-ray crystallography and NMR. *Future Med. Chem.* **2,** 1451–1468
47. Shimizu, T., Tateishi, T., Hatano, M., and Fujii-Kuriyama, Y. (1991) Probing the role of lysines and arginines in the catalytic function of cytochrome P450d by site-directed mutagenesis. Interaction with NADPH-cytochrome P450 reductase. *J. Biol. Chem.* **266,** 3372–3375
48. Lee-Robichaud, P., Akhtar, M. E., Wright, J. N., Sheikh, Q. I., and Akhtar, M. (2004) The cationic charges on Arg347, Arg358 and Arg449 of human cytochrome P450c17 (CYP17) are essential for the enzyme's cytochrome b_5-dependent acyl-carbon cleavage activities. *J. Steroid Biochem. Mol. Biol.* **92,** 119–130
49. Enoch, H. G., and Strittmatter, P. (1979) Cytochrome b_5 reduction by NADPH-cytochrome P-450 reductase. *J. Biol. Chem.* **254,** 8976–8981
50. Guengerich, F. P. (2005) Reduction of cytochrome b_5 by NADPH-cytochrome P450 reductase. *Arch. Biochem. Biophys.* **440,** 204–211
51. O'Donnell, A., Judson, I., Dowsett, M., Raynaud, F., Dearnaley, D., Mason, M., Harland, S., Robbins, A., Halbert, G., Nutley, B., and Jarman, M. (2004) Hormonal impact of the 17α-hydroxylase/C(17,20)-lyase inhibitor abiraterone acetate (CB7630) in patients with prostate cancer. *Br. J. Cancer* **90,** 2317–2325
52. Attard, G., Reid, A. H., A'Hern, R., Parker, C., Oommen, N. B., Folkerd, E., Messiou, C., Molife, L. R., Maier, G., Thompson, E., Olmos, D., Sinha, R., Lee, G., Dowsett, M., Kaye, S. B., *et al.* (2009) Selective inhibition of CYP17 with abiraterone acetate is highly active in the treatment of castration-resistant prostate cancer. *J. Clin. Oncol.* **27,** 3742–3748
53. Cojocaru, V., Winn, P. J., and Wade, R. C. (2007) The ins and outs of cytochrome P450s. *Biochim. Biophys. Acta* **1770,** 390–401
54. Lee, Y. T., Glazer, E. C., Wilson, R. F., Stout, C. D., and Goodin, D. B. (2011) Three clusters of conformational states in P450cam reveal a multistep pathway for closing of the substrate access channel. *Biochemistry* **50,** 693–703
55. Kumar, S., Davydov, D. R., and Halpert, J. R. (2005) Role of cytochrome b_5 in modulating peroxide-supported CYP3A4 activity: Evidence for a conformational transition and cytochrome P450 heterogeneity. *Drug Metab. Dispos.* **33,** 1131–1136
56. Storbeck, K. H., Swart, A. C., Fox, C. L., and Swart, P. (2015) Cytochrome b_5 modulates multiple reactions in steroidogenesis by diverse mechanisms. *J. Steroid Biochem. Mol. Biol.* **151,** 66–73
57. Pandey, A. V., and Miller, W. L. (2005) Regulation of 17,20 lyase activity by cytochrome b_5 and by serine phosphorylation of P450c17. *J. Biol. Chem.* **280,** 13265–13271
58. Geller, D. H., Auchus, R. J., and Miller, W. L. (1999) P450c17 mutations Arg-347H and R358Q selectively disrupt 17,20-lyase activity by disrupting interactions with P450 oxidoreductase and cytochrome b_5. *Mol. Endocrinol.* **13,** 167–175